# Phonon Density of States of Metallic Sn at High Pressure

Hubertus Giefers,[1] Elizabeth A. Tanis,[1] Sven P. Rudin,[2] Carl Greeff,[2] Xuezhi Ke,[1,3] Changfeng Chen,[1] Malcolm F. Nicol,[1] Michael Pravica,[1] Walter Pravica,[4] Jiyong Zhao,[5] Ahmet Alatas,[5] Michael Lerche,[5] Wolfgang Sturhahn,[5] and Ercan Alp[5]

[1]*Department of Physics and High Pressure Science and Engineering Center, University of Nevada, Las Vegas, Nevada 89154, USA*
[2]*Los Alamos National Laboratory, Los Alamos, New Mexico 87545, USA*
[3]*Department of Physics, East China Normal University, Shanghai 200062, China*
[4]*Wilbur Wright College, Chicago, Illinois 60634, USA*
[5]*Advanced Photon Source, Argonne National Laboratory, Argonne, Illinois 60439, USA*

(Received 10 April 2007; published 14 June 2007)

Determination of the lattice dynamics of Sn at high pressure has represented a major experimental challenge and eluded previous attempts. Here we report the first successful measurement of the phonon density of states of Sn at high pressure to 64 GPa using nuclear resonant inelastic x-ray scattering. We also present density functional theory calculations that are in excellent agreement with the measured data. The results of this combined experimental and theoretical study establish reliable phonon density of states of Sn at high pressure. It makes possible an accurate description of its thermodynamic properties that are of great importance and interest in high pressure research.

DOI: 10.1103/PhysRevLett.98.245502 PACS numbers: 62.50.+p, 63.20.Dj, 65.40.−b, 71.15.Mb

An important goal of condensed matter physics is to understand and predict the bonding and interatomic forces in solids. Equations of state (EOS) and structural phase transitions are important indicators of these interactions. Understanding the EOS and pressure-temperature $(p, T)$ phase diagram requires knowledge of the thermal excitation spectrum of the material in question. This information is also needed to correlate data from shock and static compression experiments [1]. The slopes of phase boundaries obey the Clausius-Clapeyron equation $dT/dP = \Delta V/\Delta S$, where $\Delta V$ and $\Delta S$ are, respectively, the volume and entropy change at the phase transition. Lattice vibrations give the dominant contribution to the entropy as well as to the thermal pressure in solids, and thus figure very prominently in the study of high pressure phase stability and EOS. Only in very few cases have the phonon spectra of materials at high pressure been measured, and generally one must resort to computational methods. Density functional theory (DFT) calculations provide frequencies of lattice vibrations that agree well with measured frequencies where direct comparisons can be made [2–5], but more comparisons are needed, especially for materials under pressure, to establish the experimental benchmarks and ensure the quality of DFT predictions. In this Letter, we present the first successful measurement of the phonon density of states (DOS) in elemental Sn at high pressure and a close comparison with DFT calculations.

The phase diagram of the Sn exhibits several phases. At ambient pressure, Sn has two polymorphic modifications. The low-temperature phase Sn-I (gray tin or $\alpha$-Sn) crystallizes in a cubic structure of the diamond type ($cF8$, $Fd$-$3m$, No. 227, $Z = 8$, $a = 6.4892$ Å at 20 °C [6]). The high-temperature phase Sn-II (white tin or $\beta$-Sn) is stable between 287–505 K. Modification II has a body-centered tetragonal (bct) structure with four atoms in the unit cell ($tI4$, $I4_1/amd$, No. 141, $Z = 4$, $a = 5.8332$ Å, $c = 3.1820$ Å at 296 K [7]). The phase transition from Sn-II to Sn-III at room temperature, widely used as a fixed point in pressure calibration, was observed at 9.4 GPa [8]. Modification III has a bct structure (bct-Sn) with two atoms in the unit cell ($tI2$, $I4/mmm$, No. 139, $Z = 2$, $a = 3.690$ Å, $c = 3.378$ Å at 296 K and 10.1 GPa [7]). The III → IV phase transition was determined at about 45 ± 5 GPa [9]. Modification IV crystallizes in a bcc structure ($cI2$, $Im$-$3m$, No. 229, $Z = 2$, $a = 3.314$ Å at 296 K and 46.5 GPa [7]) and is stable at least up to 120 GPa [9]. Shock wave studies have shown signatures of the II-III and III-liquid phase transitions [10,11].

$^{119}$Sn is the second most used Mössbauer isotope. The $^{119}$Sn resonance has been widely used at synchrotron sources since 1993 [12]. Several attempts were made to measure the phonon DOS of $\beta$-Sn [13–15]. Because of the extremely low Lamb-Mössbauer factor $f_{\mathrm{LM}}$ (4% at room temperature [13]), multiphonon processes overwhelm single-phonon process, and the phonon DOS of $\beta$-Sn could not be extracted. One attempt to overcome this problem was the measurement of $\beta$-Sn at low temperatures (100 K) [15] where $f_{\mathrm{LM}} \approx 40\%$. Another way to increase $f_{\mathrm{LM}}$ is to apply pressure. Early attempts in 1998 were made at the Advanced Photon Source (APS) with an energy resolution of 3.6 meV and without focusing at pressures of 8, 15, and 20 GPa [14]. The phonon DOS could not be extracted from those measurements.

With significantly enhanced performance of the beam lines in recent years, experiments at very high pressures on metallic Sn have become feasible. We recently carried out experiments at the European Synchrotron Radiation Facility (ESRF) at beam line ID22N and at the APS at beam line 3ID. The primary focus of this Letter is to discuss the results from the pressure series with the highest

 

pressure achieved at the APS. More details on both experimental high pressure series done at the ESRF and APS will be presented elsewhere [16].

Metallic tin enriched to 93% in $^{119}$Sn was used in the nuclear resonant inelastic x-ray scattering (NRIXS) experiments. At ambient conditions the NRIXS spectrum was recorded with the $\beta$-Sn metal piece prepared between two pieces of adhesive tape, which were then placed between two avalanche photodiode (APD) detectors. The high pressure NRIXS experiments were executed with a Paderborn-type diamond anvil cell (DAC) [17]. For measurements at 4.6 and 13.1 GPa, metallic Sn was loaded into a Be gasket. For measurements at 37 and 64 GPa, the sample was loaded in a specially designed Re gasket. A 4:1 methanol-ethanol mixture was used as a pressure transmitting medium and some spherical ruby crystals were used for pressure determination [18]. The NRIXS setup of the beam line is described in Ref. [19]. An energy range of $\pm 60$ meV for 0 and 4.6 GPa, and $\pm 70$ meV for 13.1, 37, and 64 GPa was scanned in steps of 0.25 meV. The x-ray beam was focused by two Kirkpatrick-Baez mirrors to a $7 \times 7$ $\mu$m$^2$ area impinging on the $^{119}$Sn sample in the DAC. The inelastic resonant excitations were observed by collecting the delayed $^{119}$Sn $\gamma$ quanta with two APDs placed perpendicular to the beam [17,19]. Typically, 30 to 40 NRIXS spectra, each collected in 40 min, were measured under pressure and then combined. The combined NRIXS spectra are plotted in Fig. 1. The left $y$ scale represents the actual count rate, while the right $y$ scale gives the normalization of the data by using Lipkin's sum rules [20]. Here, the first moment of the spectrum is equal to the recoil energy, $E_R = 2.575$ meV, of $^{119}$Sn. In Fig. 1(a) the overwhelming multiphonon contributions for ambient $\beta$-Sn are indicated. As tried previously [13–15], the phonon DOS matching the neutron scattering data [21] could not be extracted for the $\beta$-Sn phase. With increasing pressure multiphonon contributions decrease, which makes it possible to extract the phonon DOS from the NRIXS signal. The phonon DOS $g(E)$ of Sn in phase III and IV, derived from the measured NRIXS spectra by subtraction of multiphonon excitations and the elastic line [22], are shown in Fig. 2. As expected, the phonon energies shift evenly toward higher energies with increasing pressure. Drastic changes in the shapes of the phonon DOS between bct-Sn and bcc-Sn are not visible.

The phonon dispersion and DOS of Sn have been calculated using density functional theory methods. The vibrational frequencies were obtained by applying the direct force method [2–4,23] to results obtained from DFT calculations using the all-electron projector augmented wave (PAW) method [24] as implemented in the VASP code [25,26]. The PAW potentials included in the VASP distribution with 14 valence electrons were used. Calculations with both the generalized gradient approximation (GGA) and the local density approximation (LDA) for the exchange-correlation potential were performed using a large (54-atom) simulation cell. The total-energy convergence with

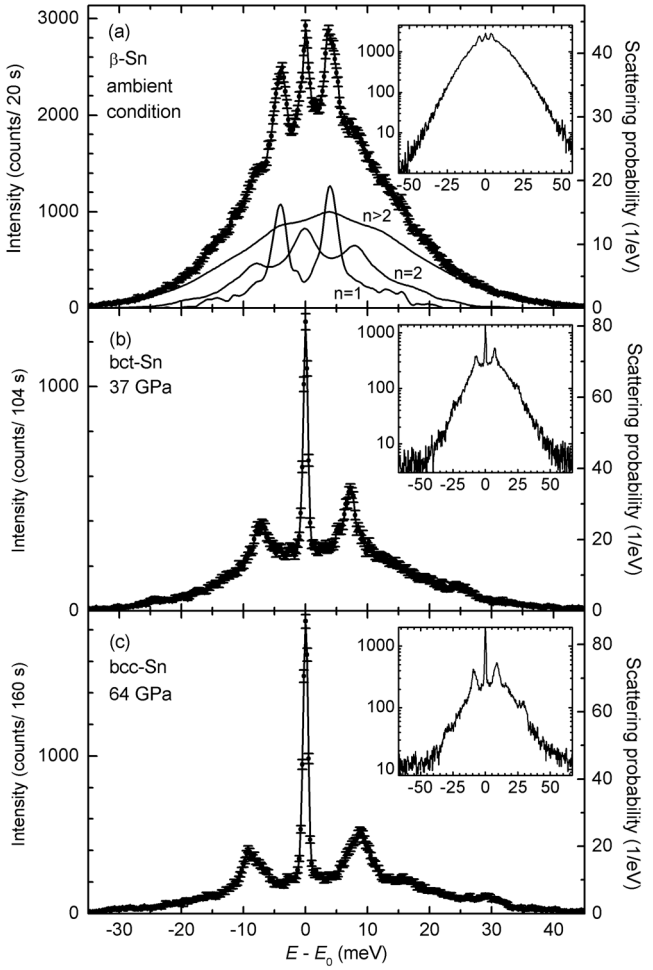


FIG. 1. Metallic $^{119}$Sn NRIXS spectra (a) at ambient conditions and (b),(c) under high pressure at 300 K. The insets show the NRIXS spectra in a logarithmic plot. In (a), the one-phonon ($n = 1$), two-phonon ($n = 2$), and $n$-phonon ($n > 2$) contributions are indicated.

respect to $k$-mesh and energy cutoff was tested. The direct force method evaluates the force constants in the simulation cell consisting of repeated unit cells (at the experimental geometry) from the forces on all atoms calculated in response to the displacement of the basis atom in one unit cell. A spatial Fourier transform with a given wave vector $q$ of the force constants results in the $q$-dependent dynamical matrix. Diagonalization of the dynamical matrix gives the corresponding frequencies. Collecting the frequencies for the wave vectors on a fine mesh in the first Brillouin zone yields the theoretical DOS. Figure 3 shows the calculated phonon dispersion and DOS at the highest (64 GPa) pressure achieved by the APS experiment. At this high pressure, multiphonon contributions are effectively suppressed, making the extracted phonon DOS highly reliable. The results provide the best experimental benchmark for comparison with the calculated results.

Since the bcc lattice has only one atom in the primitive cell, there are no optical phonon branches. In Fig. 3(b) the theoretical and experimental phonon DOS of bcc-Sn at

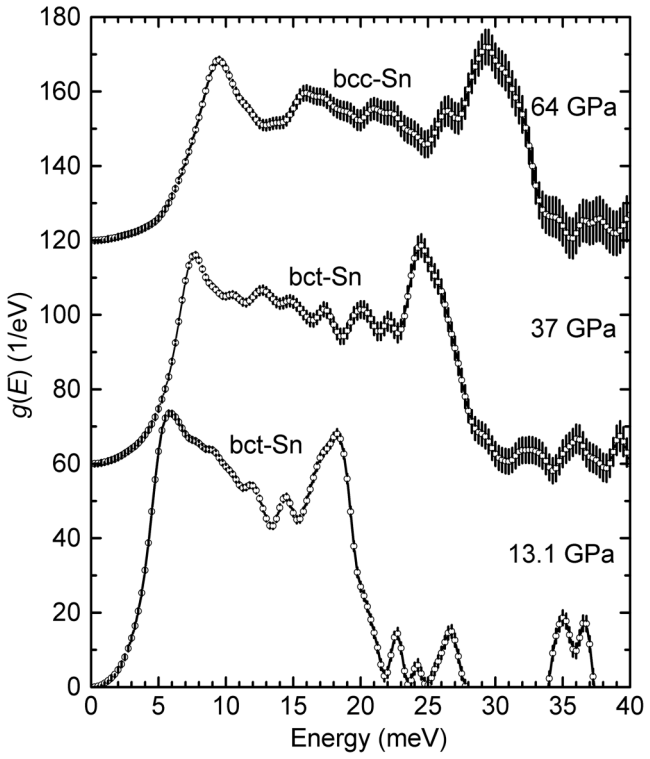


FIG. 2. Phonon DOS of Sn at high pressures at $T = 300$ K extracted from the measured NRIXS spectra after removing the contributions from multiphonon excitations and the elastic line. $g(E)$ is given on a per atom basis.

64 GPa are compared. The agreement between the calculations and the experiment is very good in both the magnitude and energies of the spectra. It is noted that the GGA calculation provides a better description at the high-frequency side. Similar agreement between experimental and theoretical DOS has also been achieved at lower pressures. The results will be presented in a forthcoming paper [16].

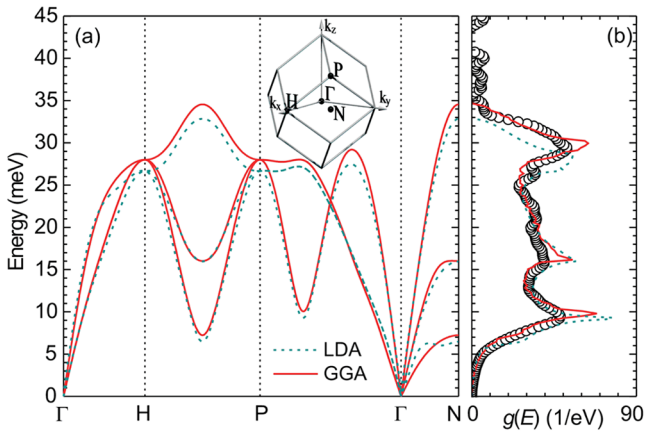


FIG. 3 (color online). (a) Theoretical phonon dispersion relation of bcc-Sn at 64 GPa. The inset shows the Brillouin zone of the bcc-Sn lattice. (b) Comparison between the theoretically calculated phonon DOS (lines) and the experimentally derived phonon DOS at 64 GPa (circles).

From the phonon DOS presented above, elastic and thermodynamic quantities important to understanding the properties of Sn can be obtained. The Lamb-Mössbauer factor $f_{\mathrm{LM}}$, the mean force constant $D_{\mathrm{mean}}$, the vibrational contributions to the Helmholtz free energy $F_{\mathrm{vib}}$, and the high-temperature Debye temperature $\Theta_{D,\mathrm{HT}}$ for Sn are calculated by integrating the corresponding experimental and theoretical partial phonon DOS $g(E)$ [cf. Figs. 4(a)–4(d)] according to the formulas in Ref. [19]. The low-temperature Debye temperature $\Theta_{D,\mathrm{LT}}$ and the Debye average phonon velocity $v_D$ are calculated from the low energy part of the phonon DOS, where the Debye approximation ($g(E) \approx E^2$) is valid. The pressure/volume data to calculate $v_D$ are taken from Refs. [7,9]. It is seen that the theoretical phonon DOS using the GGA calculation produces these quantities in better agreement with experiment at 64 GPa. For comparison at lower pressures (37 and 13.1 GPa), we only show the theoretical data obtained from the GGA calculations. The good agreement between the theory and experiment demonstrates the high quality of the measured and calculated phonon DOS over a large range of high pressure.

The Lamb-Mössbauer factor $f_{\mathrm{LM}}$ increases from ambient conditions to the highest pressure achieved in these measurements by an order of magnitude and reaches 45% at 64 GPa. It is interesting to note that the experimentally and theoretically (GGA) determined low-temperature Debye temperature $\Theta_{D,\mathrm{LT}}$ is smaller than the high-temperature Debye temperature $\Theta_{D,\mathrm{HT}}$. This is in contrast to the situation in most solids where $\Theta_{D,\mathrm{LT}}$ is typically about 10%–15% higher than $\Theta_{D,\mathrm{HT}}$. This result reveals an important feature of the lattice dynamics of Sn that must be considered in the construction of its $(p, T)$ phase diagram. From the volume dependence of $\Theta_{D,\mathrm{HT}}$ the Debye Grüneisen parameter, $\gamma_D = -(d \ln \Theta_{D,\mathrm{HT}}/d \ln V)$, is calculated. With the volume data from Refs. [7,9] the Debye Grüneisen parameter is $\gamma_D = 2.0(1)$ between 13.1 and 64 GPa, which is a normal value for simple solids.

In summary, we have performed NRIXS experiments and successfully extracted phonon density of states of Sn at high pressure to 64 GPa. This represents a major experimental advancement and fulfills a long-sought objective in high pressure materials research. Density functional theory calculations applying the direct force method give results in excellent agreement with the measured data. Based on the obtained phonon DOS, we derived several thermodynamic quantities important to understanding the lattice dynamics and construction of the $(p, T)$ phase diagram of Sn. This combined experimental and theoretical investigation establishes a reliable description of the lattice dynamics of Sn at high pressure. It also validates the theoretical methods employed here for their use in further studies of the thermodynamic properties of Sn and its compounds at high pressures.

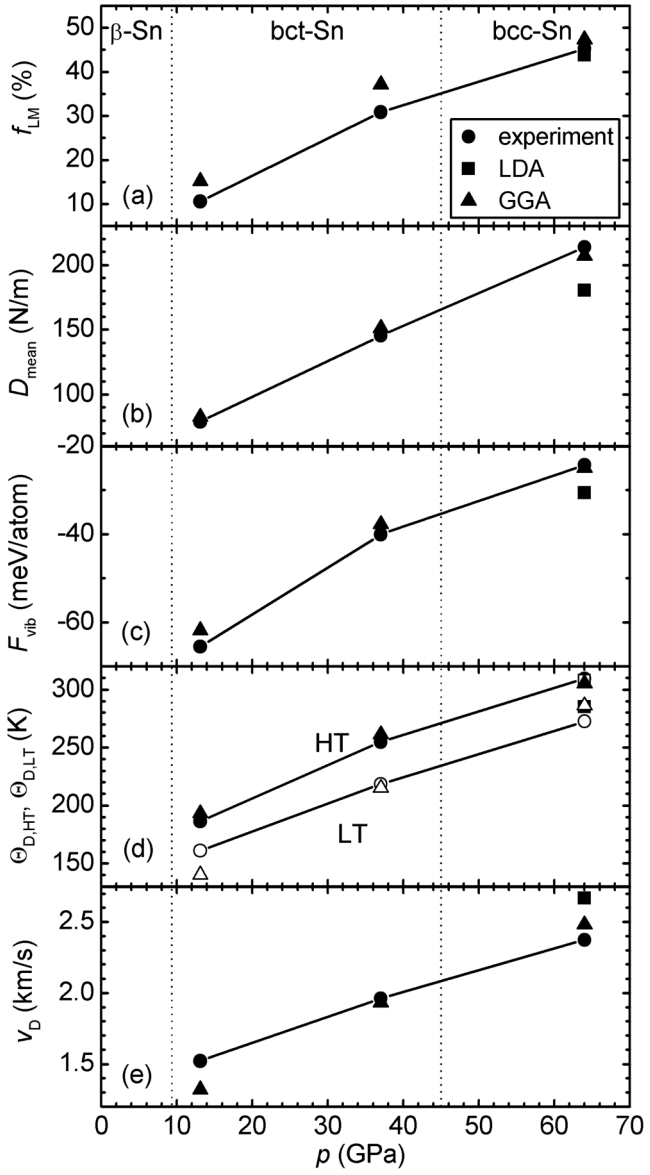


FIG. 4. Elastic and thermodynamic parameters of Sn under pressure: (a) the Lamb-Mössbauer factor $f_{\mathrm{LM}}$, (b) the mean force constant $D_{\mathrm{mean}}$, (c) the vibrational contributions to the Helmholtz free energy $F_{\mathrm{vib}}$, (d) the high- and low-temperature Debye temperature $\Theta_{D,\mathrm{HT}}$ and $\Theta_{D,\mathrm{LT}}$, and (e) the Debye average phonon velocity $v_D$. The results (symbols) are calculated using the experimental phonon DOS (circles) from Fig. 2 and the theoretical phonon DOS (square: LDA; triangles: GGA). The vertical dotted lines indicate the pressure points that separate different phases of Sn. The solid lines are guides to the eye.

The authors thank the XOR team for their technical help. The authors gratefully acknowledge support from the U.S. Department of Energy Cooperative Agreement No. DE-FC52-06NA26274 with the University of Nevada, Las Vegas. S. P. R. and C. G. are supported by the Department of Energy under Contract No. W-7405-Eng-36. HPCAT is a collaboration among the Carnegie Institution, Lawrence Livermore National Laboratory, the University of Nevada, Las Vegas, and the Carnegie/DOE Alliance Center (CDAC). Use of the Advanced Photon Source was supported by the U.S. Department of Energy, Office of Science, Office of Basic Energy Sciences, under Contract No. W-31-109-Eng-38.

[1] J. C. Boettger and D. C. Wallace, Phys. Rev. B **55**, 2840 (1997).
[2] K. Kunc and R. M. Martin, Phys. Rev. Lett. **48**, 406 (1982).
[3] S. Wei and M. Y. Chou, Phys. Rev. Lett. **69**, 2799 (1992).
[4] W. Frank, C. Elsasser, and M. Fahnle, Phys. Rev. Lett. **74**, 1791 (1995).
[5] S. P. Rudin, R. Bauer, A. Y. Liu, and J. K. Freericks, Phys. Rev. B **58**, 14 511 (1998).
[6] J. Thewlis and A. R. Davey, Nature (London) **174**, 1011 (1954).
[7] M. Liu and L.-G. Liu, High Temp. High Press. **18**, 79 (1986).
[8] V. E. Bean, S. Akimoto, P. M. Bell, S. Block, W. B. Holzapfel, M. H. Manghnani, M. F. Nicol, and S. M. Stishov, Physica (Amsterdam) **139&140B**, 52 (1986).
[9] S. Desgreniers, Y. K. Vohra, and A. L. Ruoff, Phys. Rev. B **39**, 10 359 (1989).
[10] C. Mabire and P. L. Hereil, J. Phys. IV **10**, 749 (2000).
[11] W. W. Anderson, F. Cverna, R. S. Hixson, J. Vorthman, M. D. Wilke, G. T. Gray, III, and K. L. Brown, AIP Conf. Proc. **505**, 443 (2000).
[12] E. E. Alp, T. M. Mooney, T. S. Toellner, W. Sturhahn, E. Wittho, R. Röhlsberger, E. Gerdau, H. Homma, and M. Kentjana, Phys. Rev. Lett. **70**, 3351 (1993).
[13] A. I. Chumakov, A. Barla, R. Rüffer, J. Metge, H. F. Grünsteudel, H. Grünsteudel, J. Plessel, H. Winkelmann, and M. M. Abd-Elmeguid, Phys. Rev. B **58**, 254 (1998).
[14] M. Y. Hu, Ph.D. thesis, Northwestern University, 1999.
[15] A. Barla, R. Rüffer, A. I. Chumakov, J. Metge, J. Plessel, and M. M. Abd-Elmeguid, Phys. Rev. B **61**, R14 881 (2000).
[16] H. Giefers *et al.* (unpublished).
[17] H. Giefers, R. Lübbers, K. Rupprecht, G. Wortmann, D. Alfè, and A. I. Chumakov, High Press. Res. **22**, 501 (2002).
[18] H. K. Mao, J. Xu, and P. M. Bell, J. Geophys. Res. **91**, 4673 (1986).
[19] H. Giefers, S. Koval, G. Wortmann, W. Sturhahn, E. E. Alp, and M. Y. Hu, Phys. Rev. B **74**, 094303 (2006).
[20] H. J. Lipkin, Phys. Rev. B **52**, 10 073 (1995).
[21] D. L. Price, Proc. Phys. Soc. London, Sect. A **300**, 25 (1967).
[22] W. Sturhahn, J. Phys. Condens. Matter **16**, S497 (2004).
[23] K. Parlinski, Z. Q. Li, and Y. Kawazoe, Phys. Rev. Lett. **78**, 4063 (1997).
[24] P. E. Blöchl, Phys. Rev. B **50**, 17 953 (1994).
[25] G. Kresse and J. Furthmuller, Phys. Rev. B **54**, 11 169 (1996).
[26] G. Kresse and D. Joubert, Phys. Rev. B **59**, 1758 (1999).